Uncertainty in Photoplethysmography-Based Cuffless Blood Pressure Trend Monitoring: A Personalized Approach

Mantas Rinkevičius[1], Peter H Charlton[2,3], Arūnas Lukoševičius[1], Vaidotas Marozas[1,4]

[1]Biomedical Engineering Institute, Kaunas University of Technology, Kaunas, Lithuania
[2]Department of Public Health and Primary Care, University of Cambridge, Cambridge, U.K.
[3]Research Centre for Biomedical Engineering, University of London, London, U.K.
[4]Department of Electronics Engineering, Kaunas University of Technology, Kaunas, Lithuania

Abstract

Cuffless blood pressure (BP) monitoring using photoplethysmography (PPG) is increasingly being integrated into wearables to track conditions such as hypertension. However, rather high uncertainty of continuous BP monitoring, mainly related with inter-personal variations, limits effective applications. This study aims to propose a personalized PPG analysis-based method for estimating cuffless BP and providing its uncertainty bounds. The PulseDB Vital database consisting of 2938 subjects was used. A Gaussian Process Regression model was implemented to estimate systolic and diastolic BP from PPG morphological features. Based on feature ranking, the pulse duration was found to be the most dominant predictor. The proportion of subjects with a mean absolute error < 5 mmHg was 28.80% and 60.72% for systolic and diastolic BP, respectively. The study demonstrated that the proposed approach has the potential to estimate trends of cuffless BP, especially of diastolic BP, and its prediction uncertainty.

1. Introduction

Cuffless blood pressure (BP) monitoring, which utilizes photoplethysmography (PPG) to capture volumetric blood changes, is increasingly being incorporated into wearables to track conditions such as hypertension [1, 2]. However, rather high uncertainty of continuous BP monitoring solutions, mainly related with inter-personal variations, limits effective applications. In machine learning, uncertainty refers to the lack of confidence for each prediction made by a model. While it is not possible to achieve perfect confidence, understanding and quantifying uncertainty is crucial to improving model performance and clinical decision making.

There are two types of uncertainty - epistemic and aleatoric, whereas prediction uncertainty encompasses both [3]. Epistemic or systematic uncertainty emerges when a model lacks sufficient knowledge or understanding due to limited training data [3]. To mitigate this type of uncertainty, providing more additional high-quality labeled data can be beneficial. While aleatoric also known as data or statistical uncertainty captures the inherent randomness in the system, such as sensor noise or natural variability [3]. Therefore, the poorer the quality of the data, the greater the aleatoric uncertainty.

This study aims to propose a personalized PPG analysis-based method for estimating trends of cuffless BP and providing its prediction uncertainty. The proposed approach involves the Gaussian Process Regression (GPR) method [4] for quantifying uncertainty of individual predictions.

2. Material and Methods

2.1. Data

The PulseDB Vital dataset [5] consisting of 2938 non-cardiac surgery patients was used, containing finger PPG signals and reference invasive BP measurements. The data includes patients during perioperative periods, which encompass surgical operations. The average age of the subjects was 58.76 $\pm$ 15.02 years (54.73% of male) and the body-mass index was 23.07 $\pm$ 3.53 kg/m^2. The PPG signals and continuous BP waveforms were sampled at a rate of 125 Hz, and segmented into 10-s intervals. The average duration of the subject signals was 1.38 $\pm$ 1.18 h (range 10.08 s - 9.16 h). The PulseDB Vital dataset also provides labeled fiducial points of BP measurements, which were used to obtain beat-to-beat systolic (SBP) and diastolic (DBP) BP estimates.

2.2. PPG Processing

The PPG processing algorithm for estimating BP consists of (see Figure 1): (i) PPG preprocessing, (ii) detecting PPG pulse waveforms, (iii) estimating PPG features,

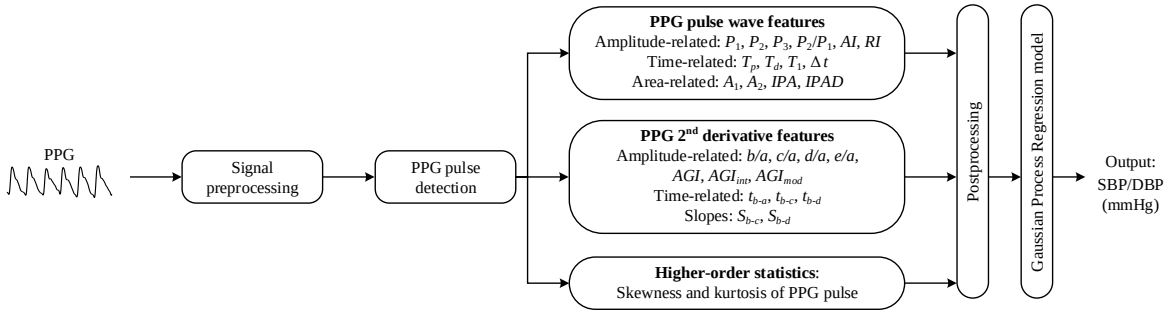

Figure 1. The block diagram of PPG processing algorithm for estimating BP.

(iv) feature postprocessing, and (v) training a GPR model to estimate SBP and DBP.

After merging 10-s intervals, the PPG signals were processed using a zero-phase fourth-order Butterworth band-pass filter with a pass-band of 0.4–7 Hz to reduce noise and improve the detectability of fiducial points. In addition, the baseline wander removal was performed using cubic spline interpolation. To identify PPG pulse waves, the mountaineer's method for peak detection was used [6].

The time intervals in which PPG features were not estimated, likely due to PPG signal morphology issues, were filled with the nearest feature value. The estimated PPG features were also postprocessed with a 20-s moving median filter to mitigate outliers and reduce aleatoric uncertainty.

2.3. PPG Feature Delineation

To estimate beat-to-beat SBP and DBP trends, 28 PPG features (see Figure 2) were assessed based on pulse morphology analysis [7,8]. The estimated PPG pulse wave features involve: (i) amplitude-related: the first and the second systolic peaks of PPG, P_1 and P_2; the diastolic peak of PPG, P_3; the ratio P_2/P_1, the reflection index (RI) - P_3/P_1; and the augmentation index (AI) - $(P_1 - P_3)/P_1$; (ii) time-related: the pulse duration, T_p; the duration of diastole, T_d; the duration of systole, T_1; the time interval from the P_1 to the P_3, Δt; (iii) area-related: the systolic area, A_1; the diastolic area, A_2; the inflection point area ratio (IPA) - A_2/A_1; the inflection point area plus the d wave amplitude of the second PPG derivative, $IPAD$.

Furthermore, the PPG second derivative features were analyzed: (i) amplitude-related: the ratios of the second PPG derivative waveform amplitudes - b/a, c/a, d/a, and e/a, the cardiovascular aging index (AGI) - $(b\text{-}c\text{-}d\text{-}e)/a$, calculated from the second PPG derivative waveform amplitudes and used for arterial stiffness estimation, the interval aging index (AGI_{int}) - $(b\text{-}e)/a$, the modified aging index (AGI_{mod}) - $(b\text{-}c\text{-}d)/a$; (ii) time-related: time intervals t_{b-a}, t_{b-c}, and t_{b-d}; (iii) slope coefficients, S_{b-c} and S_{b-d}, of the straight lines between amplitudes of b and c, and b and d waves, respectively. Additionally, two statistical features from PPG pulse waveforms were estimated – skewness, S, and kurtosis, K.

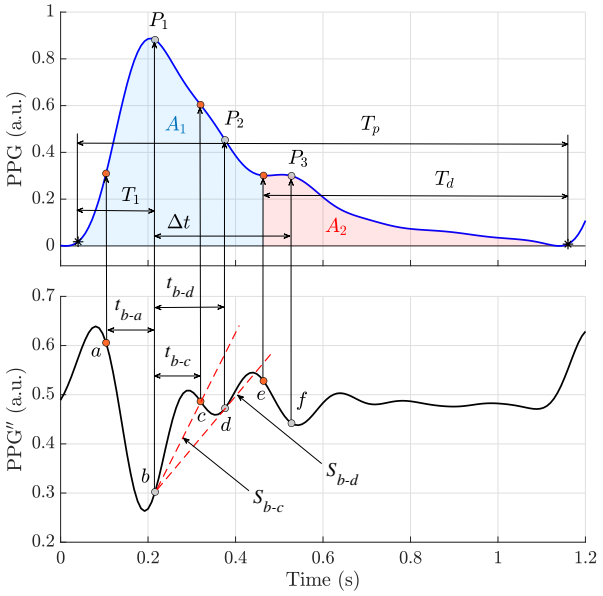

Figure 2. The PPG feature delineation based on fiducial points of the second PPG derivative, PPG″.

2.4. Feature Selection and GPR Model for BP Estimation

The PPG features for estimating BP were ranked using the Minimum Redundancy Maximum Relevance (MRMR) algorithm [9]. BP was estimated in two scenarios: (i) $-FS$ - without feature selection and using all 28 predictors, and (ii) $+FS$ - including feature selection and using the five predictors with the highest importance scores.

The hyperparameters of the GPR model were determined via a person-specific method [1] by training the model for each subject individually from simultaneous

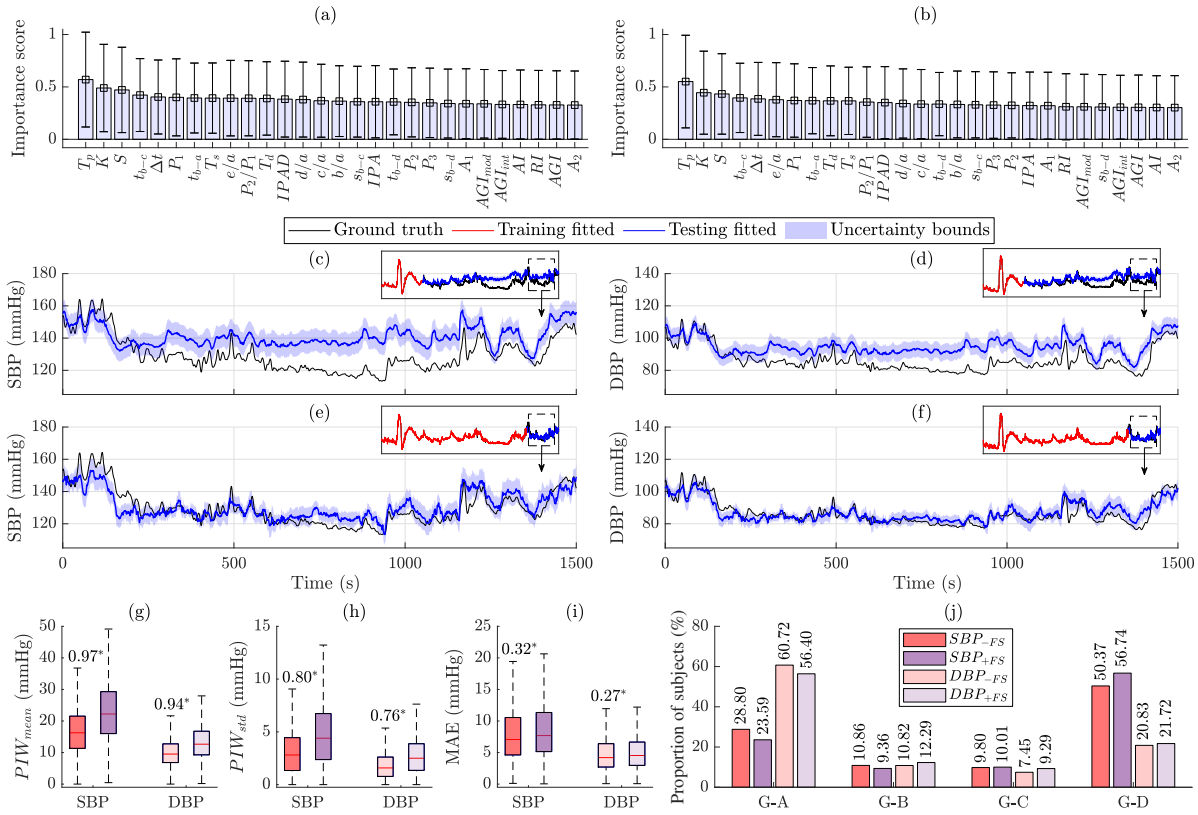

Figure 3. The importance scores of PPG features for estimating (a) SBP and (b) DBP. The example of person-specific estimated SBP and DBP trends with uncertainty bounds (95% prediction intervals) using training-testing data splits of (c-d) 1:4 and (e-f) 4:1. (g-i) The distributions of uncertainty metrics and MAE with the estimated matched-pairs r_c values between $-FS$ (without feature selection and using 28 predictors) and $+FS$ (with feature selection and using the five most important predictors) groups, when using a data split of 4:1; $p < 0.05$ is marked *. (j) The proportions of subjects grading MAE according to IEEE standard [11]: Grade A (G-A) - MAE $<$ 5 mmHg, Grade B (G-B) - 5 mmHg $\leq$ MAE $<$ 6 mmHg, Grade C (G-C) - 6 mmHg $\leq$ MAE $<$ 7 mmHg, and Grade D (G-D) - MAE $\geq$ 7 mmHg.

measurements of PPG features and cuff BP. The fully independent conditional approximation method was used to make predictions from the GPR model given the hyperparameters. The squared exponential kernel was selected for the covariance function. In addition, the limited-memory Broyden-Fletcher-Goldfarb-Shanno optimizer was used for hyperparameter estimation.

2.5. Uncertainty Evaluation and Statistical Analysis

To evaluate the performance of the implemented method, the mean absolute error (MAE) was calculated. The segment with the largest BP change was selected for training. The performance was assessed when using a training-testing data split of 4:1 in order to mitigate epistemic uncertainty (see Figure 3 (c-f)).

The uncertainty of individual predictions was quantified using 95% prediction intervals estimated by the GPR model. For this purpose, two uncertainty metrics were proposed - mean prediction interval width, PIW_{mean}, and the standard deviation of prediction interval width, PIW_{std}.

In this study, the uncertainty metrics and MAE were compared between: (i) SBP and DBP, and (ii) $-FS$ and $+FS$ predictions. The Anderson-Darling test indicated that the obtained data does not follow a Gaussian distribution. The non-parametric paired Wilcoxon signed rank test was used to test a statistical significance (α = 0.95) between analyzed distributions. Additionally, the effect size was calculated using the matched-pairs rank-biserial correlation coefficient, r_c.

3. Results

The MRMR algorithm-based feature ranking showed that the most important predictors for estimating both SBP and DBP are: the pulse duration, T_p, kurtosis, K, skewness, S, the time interval between b and c waves of the

PPG second derivative, t_{b-c}, and the time interval between systolic and diastolic peaks of the PPG, Δt (see Figure 3 (a-b)).

For DBP, the uncertainty metrics and MAE were significantly lower compared to SBP ($p < 0.01$, matched-pairs $r_c > 0.80$). Additionally, MAE grading according to IEEE standard showed that the proportion of subjects with MAE < 5 mmHg was 28.80% for SBP, and 60.72% for DBP (see Figure 3 (j)).

In terms of differences between $-FS$ and $+FS$ predictions, we can see that reducing the number of input features by using only the most important ones does not have a very large effect ($r_c < 0.50$) on MAE (see Figure 3 (i)). However, the uncertainty metrics, PIW_{mean} and PIW_{std}, tend to increase more significantly ($r_c > 0.50$) as the number of input features decreases (see Figure 3 (g-h)).

4. Discussion and Conclusion

The study aimed to propose and investigate a personalized PPG analysis-based method for estimating cuffless BP and providing its prediction uncertainty. Based on PPG feature ranking, the pulse duration, T_p, was found to be the most dominant predictor, whereas an other study [10] examined that kurtosis had the highest importance score. Our analysis also showed that pulse wave statistical features such as kurtosis and skewness were significantly relevant for estimating BP. However, it is worth emphasizing that reducing the number of model predictors could lead to a crucial increase in prediction uncertainty, despite the minimal change in performance. Therefore, the number of predictors should be chosen according to the desired confidence and accuracy of the estimation.

The performance analysis demonstrated that PPG-based estimation of DBP was more accurate and less uncertain than SBP. This could be due to factors such as pulse pressure variability and higher absolute values than those observed for DBP. The study [12] found that high DBP is more critical than SBP for predicting new-onset hypertension in younger adults with normal or high-normal BP. Therefore, robust DBP monitoring is crucial.

In this study, the hyperparameters of the model were personalized. Future work could explore population-based and hybrid approaches [1] for hyperparameter determination and benchmarking might be performed. In conclusion, the proposed method has the potential to estimate trends of cuffless BP, especially of DBP, and its prediction uncertainty.

Acknowledgments

This project was supported by the European Association of National Metrology Institutes (EURAMET) under grant agreement No. 22HLT01 (QUMPHY).

References

[1] R. Mukkamala, G. S. Stergiou, and A. P. Avolio, "Cuffless Blood Pressure Measurement," *Annu. Rev. Biomed. Eng.*, vol. 24, no. 1, pp. 203–230, Jun. 2022.

[2] C. El-Hajj and P. A. Kyriacou, "A review of machine learning techniques in photoplethysmography for the non-invasive cuff-less measurement of blood pressure," *Biomed. Signal Process. Control*, vol. 58, p. 101870, Apr. 2020.

[3] E. Hüllermeier and W. Waegeman, "Aleatoric and epistemic uncertainty in machine learning: an introduction to concepts and methods," *Mach. Learn.*, vol. 110, no. 3, pp. 457–506, Mar. 2021.

[4] E. Schulz, M. Speekenbrink, and A. Krause, "A tutorial on Gaussian process regression: Modelling, exploring, and exploiting functions," *J. Math. Psychol.*, vol. 85, pp. 1–16, Aug. 2018.

[5] W. Wang, P. Mohseni, K. L. Kilgore, and Laleh Najafizadeh, "PulseDB: A large, cleaned dataset based on MIMIC-III and VitalDB for benchmarking cuff-less blood pressure estimation methods," *Front. Digit. Health*, vol. 4, Feb. 2023.

[6] E. J. Argüello Prada and A. Paredes Higinio, "A low-complexity PPG pulse detection method for accurate estimation of the PRV during sudden decreases in the signal amplitude," *Physiol. Meas.*, vol. 41, no. 3, Feb. 2020.

[7] M. Rinkevičius, A. Rapalis, V. Pluščiauskaitė, P. Piartli, E. Kaniusas, and V. Marozas, "Low-Exertion Testing of Autonomic Cardiovascular Integrity Through PPG Signal Analysis," *CinC 2021*, Brno, Czech Republic, 2021, pp. 1-4.

[8] P. H. Charlton, P. Celka, B. Farukh, P. Chowienczyk, and J. Alastruey, "Assessing mental stress from the photoplethysmogram: a numerical study," *Physiol. Meas.*, vol. 39, no. 5, p. 054001, May 2018.

[9] C. Ding, and H. Peng, "Minimum redundancy feature selection from microarray gene expression data," *J. Bioinform. Comput. Biol.*, vol. 3, no. 2, pp. 185–205, Apr. 2005.

[10] E. Finnegan, S. Davidson, M. Harford, P. Watkinson, L. Tarassenko, and M. Villarroel, "Features from the photoplethysmogram and the electrocardiogram for estimating changes in blood pressure," *Sci. Rep.*, vol. 13, no. 1, Jan. 2023.

[11] IEEE Standard for Wearable, Cuffless Blood Pressure Measuring Devices, IEEE Std 1708a™-2019.

[12] H. Kanegae, T. Oikawa, Y. Okawara, S. Hoshide, and K. Kario., "Which blood pressure measurement, systolic or diastolic, better predicts future hypertension in normotensive young adults?," *J. Clin. Hypertens. (Greenwich)*, vol. 19, no. 6, pp. 603-610, Jun. 2017.

Address for correspondence:

Mantas Rinkevičius
Biomedical Engineering Institute, K. Baršauskas str. 59, LT-51423 Kaunas, Lithuania
mantas.rinkevicius@ktu.lt